Replacement of brain-resident myeloid cells does not alter cerebral amyloid-β deposition in mouse models of Alzheimer's disease

Nicholas H. Varvel,[1,2]* Stefan A. Grathwohl,[1]* Karoline Degenhardt,[1,2] Claudia Resch,[1,2] Andrea Bosch,[1,2] Mathias Jucker,[1,2] and Jonas J. Neher[1,2]

[1]Department of Cellular Neurology, Hertie Institute for Clinical Brain Research, University of Tübingen, 72076 Tübingen, Germany
[2]German Center for Neurodegenerative Diseases (DZNE), 72076 Tübingen, Germany

Immune cells of myeloid lineage are encountered in the Alzheimer's disease (AD) brain, where they cluster around amyloid-β plaques. However, assigning functional roles to myeloid cell subtypes has been problematic, and the potential for peripheral myeloid cells to alleviate AD pathology remains unclear. Therefore, we asked whether replacement of brain-resident myeloid cells with peripheral monocytes alters amyloid deposition in two mouse models of cerebral β-amyloidosis (APP23 and APPPS1). Interestingly, early after repopulation, infiltrating monocytes neither clustered around plaques nor showed Trem2 expression. However, with increasing time in the brain, infiltrating monocytes became plaque associated and also Trem2 positive. Strikingly, however, monocyte repopulation for up to 6 mo did not modify amyloid load in either model, independent of the stage of pathology at the time of repopulation. Our results argue against a long-term role of peripheral monocytes that is sufficiently distinct from microglial function to modify cerebral β-amyloidosis. Therefore, myeloid replacement by itself is not likely to be effective as a therapeutic approach for AD.

CORRESPONDENCE
Jonas J. Neher:
jonas.neher@uni-tuebingen.de

Abbreviations used: Aβ, amyloid-β; AD, Alzheimer's disease; GCV, ganciclovir; icv, intracerebroventricular; TK, CD11b-HSVTK.

Alzheimer's disease (AD) is a common dementing disorder characterized by deposition of the amyloid-β (Aβ) peptide, neurofibrillary tangles, and neuron loss (Holtzman et al., 2011). These pathological alterations are accompanied by a robust neuroinflammatory response, and innate immune myeloid cells are invariably found in close proximity to Aβ plaques within the AD brain (Prinz et al., 2011; Wyss-Coray and Rogers, 2012; Heneka et al., 2015). Notably, recent genome-wide association studies implicate variants of immune-related genes as risk factors for late-onset AD. These genes are expressed by myeloid cells within the brain and include, for example, *CD33*, *CR1*, and *Trem2* (Guerreiro et al., 2013; Lambert et al., 2013). This indicates an important role for myeloid cells in AD pathogenesis.

Microglia, the brain's resident macrophages, are a myeloid population that is developmentally and functionally distinct from circulating monocytes (Lavin et al., 2014; Hoeffel et al., 2015). Importantly, numerous studies have provided evidence that peripheral myeloid cells can infiltrate brain tissue and mitigate Aβ deposition (Simard et al., 2006; El Khoury et al., 2007; Town et al., 2008; Lebson et al., 2010). Furthermore, recent data indicate that infiltrating monocytes rather than resident microglia express Trem2 (Jay et al., 2015), which would further substantiate a significant role of peripheral myeloid cells in AD pathogenesis. However, distinguishing myeloid cell populations (resident vs. infiltrating) is difficult because of shared expression of marker proteins and experimental confounds associated with whole-body irradiation and bone marrow grafts, in particular blood–brain barrier permeability after irradiation (Ajami et al., 2007; Mildner et al., 2011). Thus, assessing the contribution of specific myeloid cell subtypes to AD pathology has been exceedingly difficult.

Furthermore, the accurate characterization of myeloid subtype functions in AD is particularly important in light of recent evidence suggesting

*N.H. Varvel and S.A. Grathwohl contributed equally to this paper.

The Rockefeller University Press $30.00
J. Exp. Med. 2015 Vol. 212 No. 11 1803–1809
www.jem.org/cgi/doi/10.1084/jem.20150478

that microglial dysfunction, as part of the normal aging process or as the result of pathological changes, may be a driver of AD pathology (Streit et al., 2009; Krabbe et al., 2013; Hefendehl et al., 2014). If so, the replacement of brain-resident myeloid cells with peripheral monocytes could be of therapeutic value for the treatment of AD, as indicated for other neurological disorders (Cartier et al., 2009; Derecki et al., 2012).

In this study, we therefore used our recently described central nervous system myeloid cell repopulation model (Varvel et al., 2012) to examine whether infiltrating peripheral monocytes could attenuate cerebral Aβ pathology. As expected, peripheral monocytes rapidly replaced brain-resident myeloid cells after ablation. Although infiltrating monocytes were initially distinct from brain-resident myeloid cells, over time they adopted features similar to the myeloid cells present before repopulation, such as morphology, plaque association, and Trem2 expression. Furthermore, long-term myeloid replacement did not alter Aβ deposition, arguing that under these conditions invading monocytes do not perform a long-term function in mitigating Aβ pathology that is distinct from microglia. Thus, myeloid replacement by itself is not a likely therapeutic approach for AD.

RESULTS AND DISCUSSION

Aβ deposition is not altered by myeloid cell repopulation in depositing APPPS1 mice

To investigate the effects of replacing brain-resident myeloid cells with peripheral monocytes during cerebral β-amyloidosis, we crossed APPPS1 mice, which develop first amyloid deposits at 6–8 wk of age (Radde et al., 2006), with the CD11b-HSVTK (TK) line (Heppner et al., 2005). TK mice express herpes simplex thymidine kinase in myeloid cells, which allows for myeloid cell ablation through a 2-wk intracerebroventricular (icv) ganciclovir (GCV) administration in wild-type as well as APPPS1 mice (Grathwohl et al., 2009; Varvel et al., 2012). Importantly, we have previously shown that upon discontinuation of GCV administration, peripheral monocytes repopulate the entire brain within 2 wk (either using eGFP bone marrow reconstitution or an irradiation-independent model, i.e., animals expressing red fluorescent protein under the inflammatory monocyte-specific chemokine receptor-2 promoter; Varvel et al., 2012).

3-mo-old depositing APPPS1/TK animals were subjected to 2 wk of icv GCV treatment. Histological examination of brain tissue from APPPS1/TK animals was then performed 2 wk later. As expected, APPPS1/TK$^-$ mice displayed congophilic Aβ deposits throughout the neocortex, and Iba1-positive myeloid cells were tightly clustered around these plaques (Fig. 1 a). In contrast, Iba1-positive cells in the repopulated APPPS1/TK$^+$ mice did not closely surround congophilic plaques, although some processes extending from the myeloid cells appeared to be in contact with the deposits. In addition, the morphology of the Iba1-positive cells in repopulated APPPS1/TK$^+$ mice was remarkably homogeneous throughout the cortex, with cells displaying shorter, asymmetrically oriented processes and enlarged cell bodies compared with Iba1-positive cells in APPPS1/TK$^-$ animals, regardless of their position in relation to individual Aβ plaques (Fig. 1 a). Quantitative stereological analysis further demonstrated that $\sim$2.0 × 10^6 Iba1-positive cells engrafted during the 2 wk after termination of GCV treatment, approximately double the number of microglia in the APPPS1/TK$^-$ controls (Fig. 1 c). Notably, at this early time point after repopulation, no change in congophilic amyloid or total Aβ load was detectable (Fig. 1 b).

To determine whether the continued presence of brain-engrafted monocytes would alter their responses to Aβ plaques and/or modify Aβ deposition, APPPS1/TK mice were analyzed 12 wk after GCV treatment. Again, in APPPS1/TK$^-$ animals, Iba1-positive cells clustered tightly around Aβ deposits. Interestingly, some clustering of the engrafted myeloid cells was also observed in the APPPS1/TK$^+$ animals at this later time point (Fig. 1 a), and brain sections showed $\sim$1.8 × 10^6 Iba1-positive cells in the monocyte-repopulated APPPS1/TK$^+$ mice and $\sim$1.5 × 10^6 Iba1-positive cells in the aged-matched controls (Fig. 1 c), consistent with our previous work (Varvel et al., 2012). Despite similar numbers of myeloid cells and visible responses of invading monocytes to amyloid deposits, no change in congophilic plaques or total Aβ deposits was observed at this later time point (Fig. 1 b). Furthermore, amyloid-associated dystrophic neuritic structures persisted in the myeloid cell–repopulated APPPS1/TK$^+$ mice (Fig. 1 d).

Aβ deposition is not altered by myeloid cell repopulation in depositing APP23 mice

It is possible that amyloid deposition was not altered in the APPPS1 mice because of the early and rapid nature of cerebral β-amyloidosis in this model. Therefore, we crossed TK mice to a second APP transgenic mouse model, APP23, which develops cerebral β-amyloidosis at 6–8 mo of age and shows more slowly progressing Aβ deposition in both dense cored and diffuse plaques (Sturchler-Pierrat et al., 1997).

9-mo-old APP23/TK animals were treated with GCV for 2 wk, and the mice were sacrificed 6 mo later. Histological examination of APP23/TK$^-$ control mice revealed the presence of dense core, congophilic amyloid deposits tightly surrounded by Iba1-positive myeloid cells. Strikingly, in repopulated APP23/TK$^+$ mice Iba1-positive cells also showed noticeable clustering around congophilic deposits (Fig. 1 e), although their cell bodies remained further detached from plaques than observed in TK$^-$ animals, reminiscent of results from the APPPS1 model (Fig. 1 a). Also, infiltrating monocytes remained morphologically distinct from brain-resident myeloid cells, with larger cell bodies and shorter processes (Fig. 1 e). Of note, stereological analysis revealed similar numbers of Iba1-positive cells in APP23/TK$^-$ ($\sim$1.3 × 10^6) and APP23/TK$^+$ ($\sim$1.2 × 10^6) animals (Fig. 1 g).

Despite comparable numbers of Iba1-positive cells and clustering of the invading peripheral myeloid cells around congophilic plaques in APP23/TK$^-$ and APP23/TK$^+$ animals, no changes in congophilic amyloid or total Aβ load was detectable (Fig. 1 f). Furthermore, dystrophic neuritic structures

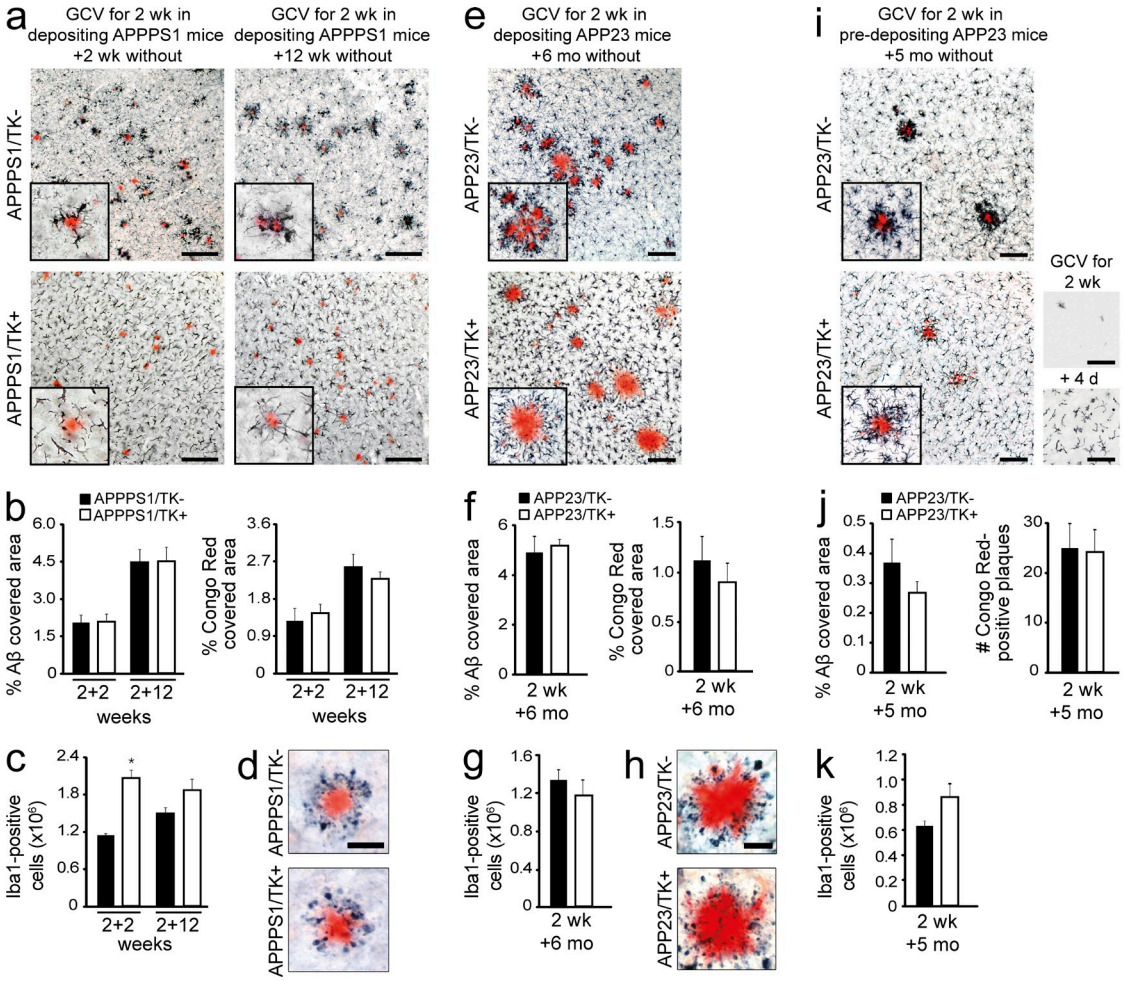

Figure 1. Long-term myeloid cell replacement does not alter Aβ deposition. Analysis of the effects of myeloid cell replacement in two APP transgenic mouse models, APPPS1 and APP23. (a) Brain-resident myeloid cells were ablated in 3-mo-old, depositing APPPS1 mice, which then remained untreated for 2 or 12 wk. Immunostaining shows Iba1-positive myeloid cells and amyloid plaques (Congo red) in APPPS1/TK$^-$ mice (top) and APPPS1/TK$^+$ mice (bottom). (b) Stereological quantification of congophilic deposits (Congo red staining) and total Aβ load (anti-Aβ staining) at 2 or 12 wk after GCV treatment in APPPS1/TK$^-$ mice compared with repopulated APPPS1/TK$^+$ animals. (c) Stereological analysis of total Iba1$^+$ cells in APPPS1/TK$^+$ compared with APPPS1/TK$^-$ mice (ANOVA: transgene × time point interaction, $F(3,25) = 6.417$, $P < 0.001$; Tukey's HSD post hoc: *, $P < 0.05$). (d) Amyloid-associated neuritic dystrophy in APPPS1/TK$^+$ and APPPS1/TK$^-$ mice (Congo red and APP staining). (e) 9-mo-old, depositing APP23/TK mice received GCV treatment and then remained untreated for 6 mo. Immunostaining shows Iba1-positive myeloid cells and amyloid plaques (Congo red). (f) Stereological quantification of congophilic deposits and total Aβ load. (g) Stereological analysis of cortical Iba1-positive cells in APP23/TK$^-$ compared with APP23/TK$^+$ mice. (h) Amyloid-associated neuritic dystrophy in APP23/TK$^+$ and APP23/TK$^-$ mice (Congo red and APP staining). (i) APP23/TK mice at 5 mo of age, i.e., before onset of plaque deposition, received GCV treatment and then remained untreated for 5 mo. Immunostaining shows Iba1-positive myeloid cells and amyloid plaques (Congo red). (bottom right, top picture) Iba1 staining after initial depletion; (bottom picture) myeloid cell morphology upon invasion. (a, e, and i) Insets show higher-magnification images. (j) Stereological quantification of total Aβ load and total number of congophilic deposits in APP23 animals. (k) Quantitative stereological analysis of Iba1-positive cells in APP23/TK$^+$ and APP23/TK$^-$ animals. Bars: (a, e, and i) 100 µm; (d and h) 50 µm. Data were pooled from at least two independent experiments. Analyses were performed in a–d for APPPS1/TK$^-$: $n = 7/8$ males and APPPS1/TK$^+$: $n = 6/5$ males for the 2+2/2+12 wk time points, respectively; in e–h for APP23/TK$^+$: $n = 4$ females, 3 males and APP23/TK$^-$: $n = 4$ females, 2 males; and i–k for APP23/TK$^+$: $n = 4$ males and APP23/TK$^-$: $n = 7$ males. Immunostainings were independently replicated at least two times. Data are presented as mean ± SEM.

persisted in the myeloid cell–repopulated mice 6 mo after termination of GCV treatment in the APP23/TK$^+$ mice (Fig. 1 j). This suggests that over the 6-mo incubation period infiltrating monocytes do not perform a function that is distinct from microglia during cerebral β-amyloidosis. Rather, with increasing time in the brain the infiltrating cells appear to become more similar to microglia, as indicated by comparable cell numbers being present in the brain (Fig. 1 g), as well as their association with amyloid plaques (Fig. 1 e).

Aβ deposition is not altered by myeloid cell repopulation in predepositing APP23 mice

To examine the possibility that myeloid cell replacement might be beneficial before the onset of Aβ deposition rather than

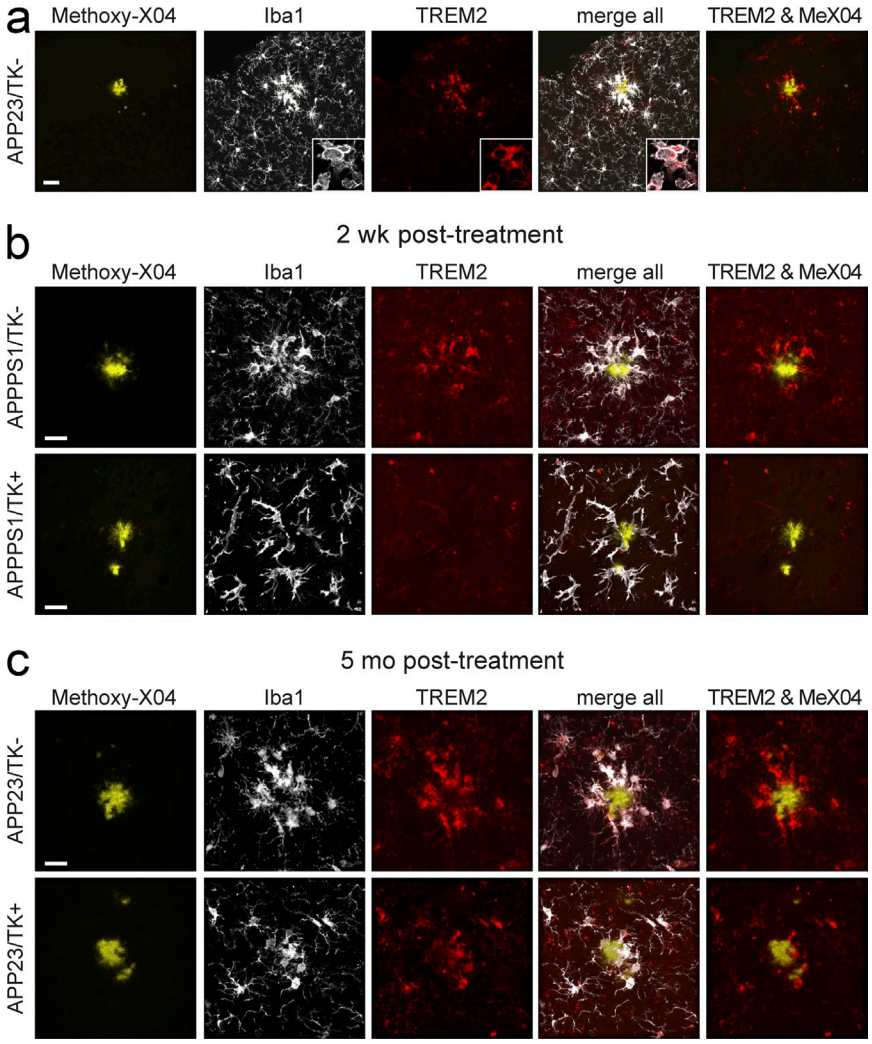

Figure 2. Trem2 expression in myeloid cells occurs with plaque association. (a) Trem2 expression is observed in myeloid cells (Iba1 positive) associated with plaques (stained with Methoxy-X04) in APP23 (shown) and APPPS1 mice (not depicted). Images are maximum projections of confocal z-stacks (insets show representative high-magnification images of a single confocal plane in plaque-associated cells). (b) Maximum projection of confocal z-stack in 4-mo-old APPPS1/TK$^-$ animals shows Iba1-positive cells expressing Trem2 in APPPS1/TK$^-$ animals, whereas nonplaque-associated infiltrating monocytes do not express Trem2 in APPPS1/TK$^+$ mice. (c) APP23/TK$^-$ as well as APP23/TK$^+$ animals repopulated before Aβ deposition show plaque-associated myeloid cells positive for Trem2 at the age of 10 mo. Bars: (a) 30 µm; (b and c) 20 µm. Immunostaining was performed for $n \geq 4$ randomly chosen animals and replicated three times.

during established cerebral β-amyloidosis, we also repopulated predepositing APP23/TK$^+$ mice at 5 mo of age. We performed this experiment only in male mice because of a later onset of Aβ deposition compared with females (Sturchler-Pierrat et al., 1997), yielding a larger time window for repopulation in the absence of Aβ deposition. We confirmed that with the same GCV administration protocol, efficient microglial ablation and brain repopulation could also be achieved in APP23 mice (Fig. 1 i). Histological analysis was performed at 10 mo of age, i.e., at early stages of plaque deposition.

Strikingly, in APP23/TK$^+$ animals repopulated before the onset of Aβ deposition, Iba1-positive cells clustered strongly around plaques, reminiscent of myeloid cells in APP23/TK$^-$ animals. Also, in plaque-free areas Iba1-positive cells in APP23/TK$^+$ animals appeared morphologically more similar to microglia, showing smaller cell bodies and a more ramified appearance than in the other repopulated groups (Fig. 1 i). Despite these similarities, no alteration of congophilic or total Aβ plaque load was observed (Fig. 1 j). Of note, the number of Iba1-positive cells was not significantly different in APP23/TK$^-$ versus APP23/TK$^+$ animals (Fig. 1 k).

TREM2 expression occurs in peripheral monocytes only after plaque association

It has recently been reported that reduced numbers of plaque-associated microglia are encountered in APP transgenic mouse models either haploinsufficient or deficient in *Trem2* (Ulrich et al., 2014; Jay et al., 2015; Wang et al., 2015). Therefore, we analyzed whether the differences in plaque association observed in our repopulated versus nonrepopulated groups could be related to Trem2 expression. In TK$^-$ animals, plaque-associated Iba1-positive cells were Trem2 immunoreactive (Fig. 2 a), in line with the findings by Jay et al. (2015). Surprisingly, early after repopulation, when infiltrating monocytes did not cluster around plaques, these cells showed no detectable Trem2 expression in APPPS1 mice (Fig. 2 b; APPPS1/TK$^+$ group 2 wk after GCV treatment discontinuation is shown). However, in long-term repopulated animals

where plaque association was evident, Iba1-positive cells clustering around amyloid deposits also showed Trem2 expression (Fig. 2 c; the APP23/TK$^+$ group repopulated at the age of 5 mo, which displayed the most pronounced plaque association, is shown). Our current data do not allow for a conclusion regarding the origin of myeloid cells (brain resident or peripheral) in control TK$^-$ mice, wherein the brain-resident myeloid cells have not been ablated; nevertheless, they indicate that Trem2 expression is induced in myeloid cells in response to the local plaque environment rather than as a result of macrophage origin.

In summary, our data suggest that in our experimental models monocytes do not perform a long-term function in the brain that is sufficiently distinct from the role of microglia to modify cerebral β-amyloidosis. These data are in line with our previous work (Varvel et al., 2012), where we reported nearly complete functional overlap between resident microglia and long-term engrafted peripheral monocytes in the measures examined, including parenchymal coverage and responses to purinergic agonists. Furthermore, monocytes invading the brain quickly down-regulated monocyte-specific markers such as, e.g., CCR2 (Varvel et al., 2012). Accordingly, it was recently shown that upon transplantation into different tissues (such as lung, spleen, and liver), bone marrow–derived macrophages show molecular reprogramming to match the resident macrophage population (Lavin et al., 2014). Thus, our work may indicate that also in the brain, the tissue environment dominates over myeloid cell origin, although more work will be needed to definitively prove this point.

A recent study used a CSF1-receptor inhibitor to deplete resident microglia and found that, in contrast to the HSVTK model, myeloid repopulation occurred from a brain-resident microglial progenitor (Elmore et al., 2014). This raises the possibility that in our long-term repopulation experiments, some peripherally derived myeloid cells may, over time, be replaced by endogenous microglial precursors. Additionally, it is possible that some of the repopulating myeloid cells may originate from the proliferation of small numbers of surviving microglia. However, the engrafted myeloid cells in our model showed clear morphological differences throughout the entire period of our experiments, whereas in the study by Elmore et al. (2014), the repopulating cells showed a ramified morphology indistinguishable from microglia. Therefore, the majority of brain-resident myeloid cells after GCV-induced microglial ablation are likely to be derived from peripheral monocytes. Strong support for this interpretation also comes from the study by Prokop et al. in this issue, where heterochronic parabiosis experiments clearly demonstrate that the repopulating cells are peripherally derived.

Our data presented here show that even during brain disease, i.e., cerebral β-amyloidosis, engrafted monocytes adopt features (such as cellular ramification, plaque association, and Trem2 expression) of brain-resident myeloid cells (be it microglia or long-term engrafted peripheral monocytes) and do not modify Aβ deposition. Therefore, myeloid replacement by itself is not a likely therapeutic option for AD or other chronic neurodegenerative diseases that are not a direct result of genetic variants in myeloid genes.

MATERIALS AND METHODS

Animals. Female hemizygous TK mice (Heppner et al., 2005) were crossed to male hemizygous APPPS1 (Radde et al., 2006) or hemizygous APP23 mice (Sturchler-Pierrat et al., 1997). APP23 mice express a transgene consisting of human APP with the KM670/671NL mutation under a Thy-1 promoter element, and APPPS1 mice carry an additional mutated human presenilin 1 (PSEN1) transgene. APPPS1 mice were generated on a C57BL/6 (B6) background, whereas APP23 and TK mice were originally derived on a B6D2 background and were backcrossed to B6 mice for >10 generations. Mice were kept under pathogen-free conditions, and experiments were in compliance with protocols approved by the local animal use and care authorities (Regierungspräsidium Tübingen).

icv GCV application. Approximately 40 h before surgery, osmotic pumps (model 2004, 0.25 µl/h; Alzet) were filled with a 50 mg/ml solution of valganciclovir (F. Hoffmann-La Roche AG) diluted in PBS and primed at 37°C. Mice were anesthetized using ketamine and xylazine (100 mg/kg ketamine, 10 mg/kg xylazine), placed on a warming pad, and secured on a modified stereotactic apparatus. The skin and the periosteum were removed and the pump reservoir was placed into a subcutaneous pocket, formed on the back of the animal. The coordinates for the cannula from bregma were +0.1 mm anteroposterior, 1.0 mm lateral, and 2.5 mm dorsoventral. The cannula (Brain Infusion kit III 1–3 mm; Alzet) was held in place by dental cement (Heraeus). After surgery, mice were treated with paracetamol (i.p. 5 mg/kg daily; Essex Pharma GmbH) for 3 d.

Removal of the osmotic pump reservoir. 2 wk after osmotic pump surgery, the animals were anesthetized using ketamine and xylazine (100 mg/kg ketamine, 10 mg/kg xylazine). A small (1 cm) incision was made in the skin between the scapulae to gain access to the subcutaneous pump reservoir and tube connecting the pump reservoir to the head cannula. The connecting tube was cut, and the pump reservoir was removed. The cannula and the attached tube were left in place, and the free end of the tube was sealed with dental cement. The incision was closed with sutures and the animal was returned to its cage. After surgery, mice were treated with acetaminophen (i.p. 5 mg/kg daily; Essex Pharma GmbH) for 3 d.

Histology. After transcardial perfusion, brains were removed and the hemisphere contralateral to the implanted cannula was fresh frozen for biochemical analysis. The hemisphere that received cannula insertion was fixed in 4% PFA for 24 h, followed by cryoprotection in 30% sucrose in PBS. Brains were subsequently frozen in 2-methylbutane and coronally sectioned at 40 µm using a freezing-sliding microtome. Immunohistochemical stainings were performed using the VECTASTAIN Elite ABC kits (Vector Laboratories). The following primary antibodies were used: rabbit polyclonal antibody to ionized calcium binding adapter molecule 1 (Iba1; Wako Pure Chemical Industries), rabbit polyclonal antibody to human Aβ (CN3), and rabbit polyclonal antibody 5313 to the N terminus of APP (as a marker of dystrophic neurites; provided by C. Haass, Ludwig Maximilians University Munich, Munich, Germany). All antibodies were used at a dilution of 1:2,000. Congo red staining was performed according to standard laboratory procedures. Images were acquired on an Axioplan 2 microscope with AxioCam MRm, using a 20×/0.5 air objective and AxioVision 4.7 software (all from Carl Zeiss).

For immunofluorescence staining, sections were prepared as in the previous paragraph, blocked for 1 h with 5% goat serum, and incubated overnight, at 4°C, with antibodies against rabbit anti-Iba1 (1:2,000; Wako Pure Chemical Industries) and sheep anti-TREM2 (1:100; R&D Systems). Please note that this antibody was established by Jay et al. (2015) to be specific for murine Trem2 (as indicated by lack of staining in Trem2$^{-/-}$ animals). Primary antibody incubation was followed by extensive washing and incubation with anti–sheep–Alexa Fluor 546 and anti–rabbit–Alexa Fluor 647 secondary

antibodies (Jackson ImmunoResearch Laboratories, Inc.). Plaques were then counterstained with Methoxy-X04 (4% vol of 10 mg/ml Methoxy-X04 in dimethyl sulfoxide and 7.7% vol Cremophor EL in PBS) and sections washed extensively. Images were acquired with an LSM 510 META (Axiovert 200M) confocal microscope using a 63× oil objective (1.4 NA) and LSM software 4.2 (all from Carl Zeiss). Laser lines 405, 543, and 633 were used to sequentially excite the fluorophores, and z-stacks of 17-µm thickness were acquired (1-µm intervals). Maximum-intensity projections were created using IMARIS 7.7.2 software (Bitmap).

Stereological assessment of amyloid load and Iba1 cell number. Numbers of Iba1-positive cells and Aβ load were assessed on random sets of every 12th systematically sampled 40-µm-thick sections through the neocortex typically yielding 8–10 sections/mouse. Analysis was performed with the aid of the Stereologer software (Stereo Investigator 6; MBF Bioscience) and a motorized x-y-z stage coupled to a video microscopy system (Microfire color microscope camera; Optronics). For Iba1 quantification, the optical fractionator technique was used with three-dimensional dissectors (area 495 × 495 μm^2, height 15 µm, guard height 2 µm, counting frame 50 × 50 μm^2). Iba1-positive cells with complete soma within the dissector volume were counted (Grathwohl et al., 2009; Varvel et al., 2012). Congophilic amyloid and Aβ load was analyzed using the area fraction technique (Bondolfi et al., 2002).

Statistical analysis. Statistical analysis was performed using JMP 7.1 software. The results are expressed as mean values ± SEM. Student's *t* test was used for comparison of two groups, and two-way ANOVA was used for comparison of multiple groups followed by Tukey's HSD post hoc analysis.

We thank Dr. Adriano Aguzzi (University of Zurich, Zurich, Switzerland) for kindly providing the HSVTK mouse line and J. Odenthal for experimental help and advice.

This work was supported by the Alzheimer's Association (N.H. Varvel), The Alexander von Humboldt Foundation (N.H. Varvel), and a Roman Herzog Postdoctoral Fellowship of the Hertie Foundation (J.J. Neher).

The authors declare no competing financial interests.

Submitted: 16 March 2015
Accepted: 11 September 2015

REFERENCES

Ajami, B., J.L. Bennett, C. Krieger, W. Tetzlaff, and F.M.V. Rossi. 2007. Local self-renewal can sustain CNS microglia maintenance and function throughout adult life. *Nat. Neurosci.* 10:1538–1543. http://dx.doi.org/10.1038/nn2014

Bondolfi, L., M. Calhoun, F. Ermini, H.G. Kuhn, K.-H. Wiederhold, L. Walker, M. Staufenbiel, and M. Jucker. 2002. Amyloid-associated neuron loss and gliogenesis in the neocortex of amyloid precursor protein transgenic mice. *J. Neurosci.* 22:515–522.

Cartier, N., S. Hacein-Bey-Abina, C.C. Bartholomae, G. Veres, M. Schmidt, I. Kutschera, M. Vidaud, U. Abel, L. Dal-Cortivo, L. Caccavelli, et al. 2009. Hematopoietic stem cell gene therapy with a lentiviral vector in X-linked adrenoleukodystrophy. *Science.* 326:818–823. http://dx.doi.org/10.1126/science.1171242

Derecki, N.C., J.C. Cronk, Z. Lu, E. Xu, S.B.G. Abbott, P.G. Guyenet, and J. Kipnis. 2012. Wild-type microglia arrest pathology in a mouse model of Rett syndrome. *Nature.* 484:105–109. http://dx.doi.org/10.1038/nature10907

El Khoury, J., M. Toft, S.E. Hickman, T.K. Means, K. Terada, C. Geula, and A.D. Luster. 2007. Ccr2 deficiency impairs microglial accumulation and accelerates progression of Alzheimer-like disease. *Nat. Med.* 13:432–438. http://dx.doi.org/10.1038/nm1555

Elmore, M.R., A.R. Najafi, M.A. Koike, N.N. Dagher, E.E. Spangenberg, R.A. Rice, M. Kitazawa, B. Matusow, H. Nguyen, B.L. West, and K.N. Green. 2014. Colony-stimulating factor 1 receptor signaling is necessary for microglia viability, unmasking a microglia progenitor cell in the adult brain. *Neuron.* 82:380–397. http://dx.doi.org/10.1016/j.neuron.2014.02.040

Grathwohl, S.A., R.E. Kälin, T. Bolmont, S. Prokop, G. Winkelmann, S.A. Kaeser, J. Odenthal, R. Radde, T. Eldh, S. Gandy, et al. 2009. Formation and maintenance of Alzheimer's disease β-amyloid plaques in the absence of microglia. *Nat. Neurosci.* 12:1361–1363. http://dx.doi.org/10.1038/nn.2432

Guerreiro, R., A. Wojtas, J. Bras, M. Carrasquillo, E. Rogaeva, E. Majounie, C. Cruchaga, C. Sassi, J.S.K. Kauwe, S. Younkin, et al. Alzheimer Genetic Analysis Group. 2013. TREM2 variants in Alzheimer's disease. *N. Engl. J. Med.* 368:117–127. http://dx.doi.org/10.1056/NEJMoa1211851

Hefendehl, J.K., J.J. Neher, R.B. Sühs, S. Kohsaka, A. Skodras, and M. Jucker. 2014. Homeostatic and injury-induced microglia behavior in the aging brain. *Aging Cell.* 13:60–69. http://dx.doi.org/10.1111/acel.12149

Heneka, M.T., D.T. Golenbock, and E. Latz. 2015. Innate immunity in Alzheimer's disease. *Nat. Immunol.* 16:229–236. http://dx.doi.org/10.1038/ni.3102

Heppner, F.L., M. Greter, D. Marino, J. Falsig, G. Raivich, N. Hövelmeyer, A. Waisman, T. Rülicke, M. Prinz, J. Priller, et al. 2005. Experimental autoimmune encephalomyelitis repressed by microglial paralysis. *Nat. Med.* 11:146–152. http://dx.doi.org/10.1038/nm1177

Hoeffel, G., J. Chen, Y. Lavin, D. Low, F.F. Almeida, P. See, A.E. Beaudin, J. Lum, I. Low, E.C. Forsberg, et al. 2015. C-Myb$^+$ erythro-myeloid progenitor-derived fetal monocytes give rise to adult tissue-resident macrophages. *Immunity.* 42:665–678.

Holtzman, D.M., J.C. Morris, and A.M. Goate. 2011. Alzheimer's disease: the challenge of the second century. *Sci. Transl. Med.* 3:77sr1. http://dx.doi.org/10.1126/scitranslmed.3002369

Jay, T.R., C.M. Miller, P.J. Cheng, L.C. Graham, S. Bemiller, M.L. Broihier, G. Xu, D. Margevicius, J.C. Karlo, G.L. Sousa, et al. 2015. TREM2 deficiency eliminates TREM2$^+$ inflammatory macrophages and ameliorates pathology in Alzheimer's disease mouse models. *J. Exp. Med.* 212:287–295. http://dx.doi.org/10.1084/jem.20142322

Krabbe, G., A. Halle, V. Matyash, J.L. Rinnenthal, G.D. Eom, U. Bernhardt, K.R. Miller, S. Prokop, H. Kettenmann, and F.L. Heppner. 2013. Functional impairment of microglia coincides with Beta-amyloid deposition in mice with Alzheimer-like pathology. *PLoS ONE.* 8:e60921. http://dx.doi.org/10.1371/journal.pone.0060921

Lambert, J.-C., C.A. Ibrahim-Verbaas, D. Harold, A.C. Naj, R. Sims, C. Bellenguez, A.L. DeStafano, J.C. Bis, G.W. Beecham, B. Grenier-Boley, et al. Cohorts for Heart and Aging Research in Genomic Epidemiology. 2013. Meta-analysis of 74,046 individuals identifies 11 new susceptibility loci for Alzheimer's disease. *Nat. Genet.* 45:1452–1458. http://dx.doi.org/10.1038/ng.2802

Lavin, Y., D. Winter, R. Blecher-Gonen, E. David, H. Keren-Shaul, M. Merad, S. Jung, and I. Amit. 2014. Tissue-resident macrophage enhancer landscapes are shaped by the local microenvironment. *Cell.* 159:1312–1326. http://dx.doi.org/10.1016/j.cell.2014.11.018

Lebson, L., K. Nash, S. Kamath, D. Herber, N. Carty, D.C. Lee, Q. Li, K. Szekeres, U. Jinwal, J. Koren, et al. 2010. Trafficking CD11b-positive blood cells deliver therapeutic genes to the brain of amyloid-depositing transgenic mice. *J. Neurosci.* 30:9651–9658. http://dx.doi.org/10.1523/JNEUROSCI.0329-10.2010

Mildner, A., B. Schlevogt, K. Kierdorf, C. Böttcher, D. Erny, M.P. Kummer, M. Quinn, W. Brück, I. Bechmann, M.T. Heneka, et al. 2011. Distinct and non-redundant roles of microglia and myeloid subsets in mouse models of Alzheimer's disease. *J. Neurosci.* 31:11159–11171. http://dx.doi.org/10.1523/JNEUROSCI.6209-10.2011

Prinz, M., J. Priller, S.S. Sisodia, and R.M. Ransohoff. 2011. Heterogeneity of CNS myeloid cells and their roles in neurodegeneration. *Nat. Neurosci.* 14:1227–1235. http://dx.doi.org/10.1038/nn.2923

Prokop, S., K.R. Miller, N. Drost, S. Handrick, V. Mathur, J. Luo, A. Wegner, T. Wyss-Coray, and F.L. Heppner. 2015. Impact of peripheral myeloid cells on amyloid-β pathology in Alzheimer's disease–like mice. *J. Exp. Med.* 212. http://dx.doi.org/10.1084/jem.20150479

Radde, R., T. Bolmont, S.A. Kaeser, J. Coomaraswamy, D. Lindau, L. Stoltze, M.E. Calhoun, F. Jäggi, H. Wolburg, S. Gengler, et al. 2006. Aβ42-driven cerebral amyloidosis in transgenic mice reveals early and robust pathology. *EMBO Rep.* 7:940–946. http://dx.doi.org/10.1038/sj.embor.7400784

Simard, A.R., D. Soulet, G. Gowing, J.-P. Julien, and S. Rivest. 2006. Bone marrow-derived microglia play a critical role in restricting senile plaque

formation in Alzheimer's disease. *Neuron*. 49:489–502. http://dx.doi.org/10.1016/j.neuron.2006.01.022

Streit, W.J., H. Braak, Q.-S. Xue, and I. Bechmann. 2009. Dystrophic (senescent) rather than activated microglial cells are associated with tau pathology and likely precede neurodegeneration in Alzheimer's disease. *Acta Neuropathol.* 118:475–485. http://dx.doi.org/10.1007/s00401-009-0556-6

Sturchler-Pierrat, C., D. Abramowski, M. Duke, K.H. Wiederhold, C. Mistl, S. Rothacher, B. Ledermann, K. Bürki, P. Frey, P.A. Paganetti, et al. 1997. Two amyloid precursor protein transgenic mouse models with Alzheimer disease-like pathology. *Proc. Natl. Acad. Sci. USA*. 94:13287–13292. http://dx.doi.org/10.1073/pnas.94.24.13287

Town, T., Y. Laouar, C. Pittenger, T. Mori, C.A. Szekely, J. Tan, R.S. Duman, and R.A. Flavell. 2008. Blocking TGF-β–Smad2/3 innate immune signaling mitigates Alzheimer-like pathology. *Nat. Med.* 14:681–687. http://dx.doi.org/10.1038/nm1781

Ulrich, J.D., M.B. Finn, Y. Wang, A. Shen, T.E. Mahan, H. Jiang, F.R. Stewart, L. Piccio, M. Colonna, and D.M. Holtzman. 2014. Altered microglial response to Aβ plaques in APPPS1-21 mice heterozygous for TREM2. *Mol. Neurodegener.* 9:20. http://dx.doi.org/10.1186/1750-1326-9-20

Varvel, N.H., S.A. Grathwohl, F. Baumann, C. Liebig, A. Bosch, B. Brawek, D.R. Thal, I.F. Charo, F.L. Heppner, A. Aguzzi, et al. 2012. Microglial repopulation model reveals a robust homeostatic process for replacing CNS myeloid cells. *Proc. Natl. Acad. Sci. USA*. 109:18150–18155. http://dx.doi.org/10.1073/pnas.1210150109

Wang, Y., M. Cella, K. Mallinson, J.D. Ulrich, K.L. Young, M.L. Robinette, S. Gilfillan, G.M. Krishnan, S. Sudhakar, B.H. Zinselmeyer, et al. 2015. TREM2 lipid sensing sustains the microglial response in an Alzheimer's disease model. *Cell.* 160:1061–1071. http://dx.doi.org/10.1016/j.cell.2015.01.049

Wyss-Coray, T., and J. Rogers. 2012. Inflammation in Alzheimer disease-a brief review of the basic science and clinical literature. *Cold Spring Harb. Perspect. Med.* 2:a006346. http://dx.doi.org/10.1101/cshperspect.a006346